SCIENCE CHINA
Technological Sciences

• Article •

January 2015 Vol.58 No.1: 56–63
doi: 10.1007/s11431-014-5667-1

A simple compliance modeling method for flexure hinges

ZHU ZhiWei, ZHOU XiaoQin*, WANG RongQi & LIU Qiang

School of Mechanical Science and Engineering, Jilin University, Changchun 130022, China

Received June 24, 2014; accepted September 1, 2014; published online October 24, 2014

Various types of flexure hinges have been introduced and implemented in a variety of fields due to their superior performances. The Castigliano's second theorem, the Euler–Bernoulli beam theory based direct integration method and the unit-load method have been employed to analytically describe the elastic behavior of flexure hinges. However, all these methods require prior-knowledge of the beam theory and need to execute laborious integration operations for each term of the compliance matrix, thus highly decreasing the modeling efficiency and blocking practical applications of the modeling methods. In this paper, a novel finite beam based matrix modeling (FBMM) method is proposed to numerically obtain compliance matrices of flexure hinges with various shapes. The main concept of the method is to treat flexure hinges as serial connections of finite micro-beams, and the shearing and torsion effects of the hinges are especially considered to enhance the modeling accuracy. By means of matrix calculations, complete compliance matrices of flexure hinges can be derived effectively in one calculation process. A large number of numerical calculations are conducted for various types of flexure hinges with different shapes, and the results are compared with the ones obtained by conventional modeling methods. It demonstrates that the proposed modeling method is not only efficient but also accurate, and it is a more universal and more robust tool for describing elastic behavior of flexure hinges.

flexure hinge, compliance matrix, finite beam based matrix modeling, modeling accuracy

Citation: Zhu Z W, Zhou X Q, Wang R Q, et al. A simple compliance modeling method for flexure hinges. Sci China Tech Sci, 2015, 58: 56–63, doi: 10.1007/s11431-014-5667-1

1 Introduction

Flexure hinges, serving as the substitutions of conventional joints, have been extensively employed in micro mechanical systems to obtain friction and lubrication free motions with high resolution, high precision and small structure sizes. Typical implementations can be found in micro-machining systems [1,2], micro/nano manipulators [3,4], and micro/nano positioning stages [5,6]. Up to date, various types of flexure hinges with different shapes and moving features have been introduced, such as right circular flexure hinges [7], leaf-spring flexure hinges [8,9], elliptical-arc-fillet flexure hinges [10,11], V-shaped flexure hinges [12,13], conic flexure hinges [14–16], power function shaped flexure hinges [17], fillet flexure hinges [8,18,19], annulus-shaped flexure hinges [20,21], flexure hinges with freeform shapes [22,23] and so on. Developments of these types of flexure hinges will add more feasibility and flexibility to the design of flexural mechanisms, however, it will simultaneously rise difficulties for the design and optimization processes due to the complicated shapes of the flexure hinges which are usually hard to be accurately modeled [24,25].

Discussions of properties and analytical models of flexure hinges have been a long history [26–28]. To obtain accurate models of the elastic deformation behavior of the notched flexure hinges and accordingly have good estimations of moving features of the mechanisms, various efforts have been devoted by researchers to modeling the basic

*Corresponding author (email: xqzhou@jlu.edu.cn)

compliances of the flexure hinges [7,11,27]. Currently, the Castigliano's second theorem [8,13,15], the Euler–Bernoulli beam theory based direct integration method [10,14,18] and the unit-load method [17] are the three commonly used methods for analytically modeling the compliances of flexure hinges. Although closed-form compliance equations can be obtained through these methods, each term of the complete compliance matrix needs to be separately executed by laborious integral operations over the entire flexure length, significantly decreasing the modeling efficiency [29]. Besides, the modeling methods require prior-knowledge of the beam theory, blocking practical implementations in the industry.

To avoid tedious mathematical descriptions of the compliance equations which are generally not concise enough for practical applications, high order polynomial approximation methods were employed to obtain empirical equations or dimensionless design graphs of certain sorts of flexure hinges [12,20,25]. Recently, great efforts have been focused on obtaining the generalized compliance models, and the generalized equations for the family of elliptical-arc-fillet flexure hinges and the family of conic-section flexure hinges have been introduced by means of unifying mathematical descriptions of the geometric shapes of the hinges [14,18,30,31]. However, as for certain flexure hinges with totally different dominant features, to obtain the unified mathematical descriptions seems to be difficult and even impossible. Thus, no universal compliance equations for flexure hinges with various shapes can be obtained, it is crucial to develop more universal and efficient modeling methods for flexure hinges, especially for the newly developed ones.

In this paper, a novel finite beam based matrix modeling (FBMM) method is proposed to numerically obtain compliance matrices of flexure hinges with complicated shapes. Comparing with conventional modeling methods, the main advantages of the FBMM can be summarized as follows: 1) It requires no knowledge of the beam theory and even the calculus, well extending practical applications of the FBMM; 2) terms of the complete compliance matrix can be obtained during one calculation process by simple matrix operation; 3) since matrix based calculation can be conducted more efficiently and accurately by computers [9, 32–34], the proposed modeling method will be very promising for facilitating computer-aided-design of flexure hinges; 4) in view of the modeling principle, compliance matrices of hinges with any shapes can be simply and directly obtained, even the ones described by discrete points.

2 Compliance modeling

Generally, in view of the shapes of the central axis, the flexure hinges can be categorized into two sorts, namely the circular- axis flexure hinges as shown in Figure 1(a) and the straight-axis flexure hinges. As for the straight-axis flexure hinges, they can be further categorized into two sorts from the view of notch shapes, namely the single-directional flexure hinge with variable width as shown in Figure 1(b), and the bi-directional flexure hinge with both variable width and variable thickness as shown in Figure 1(c).

As shown in Figure 1, the *o-xyz* denotes the global Car-

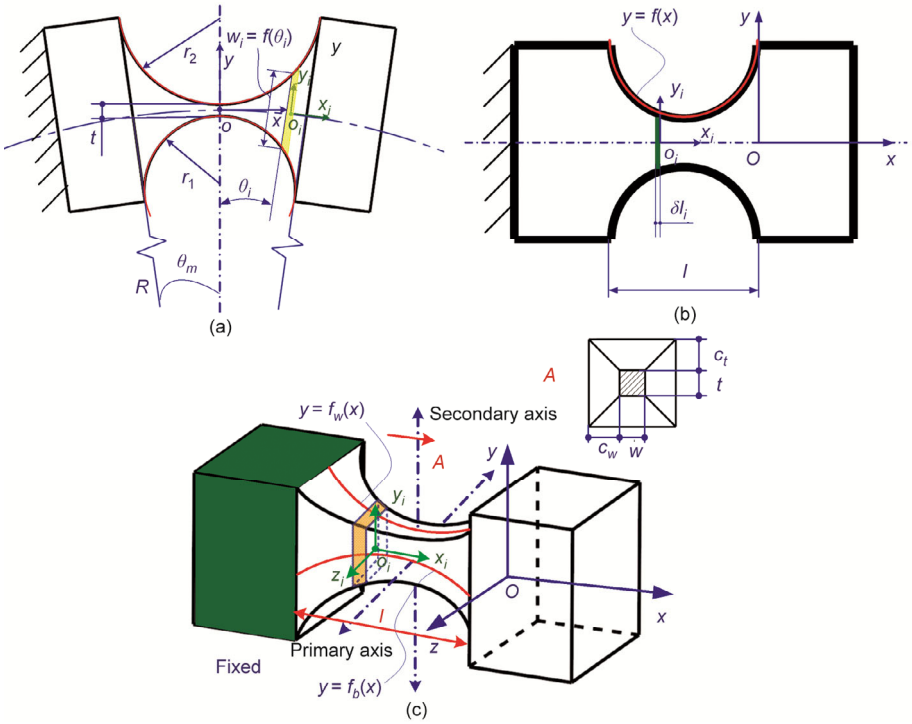

Figure 1 Schematic of typical flexure hinges. (a) Circular-axis hinge; (b) single-directional hinge; (c) bi-directional hinge.

tesian coordinate of the flexure hinges. As for the circular-axis flexure hinges shown in Figure 1(a), the shape of this sort of flexure hinges can be determined by the median radius R, the center angle θ_m, and the radius of the two circle curves r_1 and r_2. $y=f(\theta)$ denotes the mathematical description of the distance between the upper and the lower curves of the flexure hinges, respectively. For more details about the geometry and the mathematical descriptions, one can refer to ref. [35]. As for the straight-axis flexure hinges shown in Figures 1(b) and (c), l represents the total length of the notch; $y=f_w(x)$ and $z=f_b(x)$ denote the mathematical descriptions of the outer curves along the x-axis and the z-axis in the global coordinate frame, respectively.

During the modeling, each sort of the flexure hinges will be uniformly divided into N pieces, and each piece can be treated as a micro Euler–Bernoulli beam with rectangular cross-section. The o_i–$x_iy_iz_i$ denotes the local Cartesian coordinate of the i-th micro- beam as shown in Figure 1. Overall, with the assumption that the effects of stress distributions on elastic deformations of flexure hinges can be ignored, each sort of the flexure hinges will be regarded as series connections of all the micro-beams. Based on the matrix based modeling method, the compliance of the flexure hinge in the global coordinate can be expressed by [1, 34]

$$\boldsymbol{C}=\sum_{i=1}^{N}\boldsymbol{T}_i\boldsymbol{C}_i^{(\mathrm{L})}\boldsymbol{T}_i^{\mathrm{T}}, \tag{1}$$

where $\boldsymbol{T}_i$ denotes the compliance transformation matrix (CTM), $\boldsymbol{C}_i^{(\mathrm{L})}$ denotes compliance matrix of the i-th single micro-beam in its local coordinate which has been proposed and widely employed for describing the elastic deformation behavior of the leaf-spring flexure hinges [9,36]. However, the complex shear effects are often ignored or simplified in these researches. Thus, to enhance the modeling accuracy, a modified version for the compliance matrix of the micro-beam is derived by

$$\boldsymbol{C}_i^{(\mathrm{L})}=\begin{bmatrix}
\frac{L}{Eb_iw_i} & 0 & 0 & 0 & 0 & 0\\
0 & \frac{4L^3}{Eb_iw_i^3}+\frac{\alpha_sL}{Gb_iw_i} & 0 & 0 & 0 & \frac{6L^2}{Eb_iw_i^3}\\
0 & 0 & \frac{4L^3}{Eb_i^3w_i}+\frac{\alpha_sL}{Gb_iw_i} & 0 & -\frac{6L^2}{Eb_i^3w_i} & 0\\
0 & 0 & 0 & C_{\theta_x,M_x} & 0 & 0\\
0 & 0 & -\frac{6L^2}{Eb_i^3w_i} & 0 & \frac{12L}{Eb_i^3w_i} & 0\\
0 & \frac{6L^2}{Eb_iw_i^3} & 0 & 0 & 0 & \frac{12L}{Eb_iw_i^3}
\end{bmatrix}, \tag{2}$$

where E and G are the modulus of elasticity and the modulus of rigidity, respectively. b_i and w_i denote the cross- section dimensions of the i-th micro-beam, L denotes the length of the micro-beam, and α_s is the shear coefficient of the material. With μ being the Poisson ratio, the shear coefficient α_s introduced by Cowper for the micro-beams with rectangular cross-section is employed [37]:

$$\alpha_s=\frac{12+11\mu}{10(1+\mu)}. \tag{3}$$

To accurately describe the torsion behavior of the micro-beam, a newly developed torsion compliance which is thickness-to-width ratio independent is employed with the definition of the ratio $z_i=b_i/w_i$ [38]:

$$C_{\theta_x,M_x}=\frac{7L}{2G}\left(\frac{1}{w_ib_i^3}+\frac{1}{w_i^3b_i}\right)\frac{z_i^2+2.609z_i+1}{1.17z_i^2+2.191z_i+1.17}. \tag{4}$$

Referring to eq. (1), the CTM $\boldsymbol{T}_i$ takes on the following form [9, 32–34, 39]:

$$\boldsymbol{T}_i=\begin{bmatrix}\boldsymbol{R}_i(\phi) & \boldsymbol{S}_i(\boldsymbol{r}_i)\boldsymbol{R}_i(\phi)\\ \boldsymbol{O} & \boldsymbol{R}_i(\phi)\end{bmatrix}, \tag{5}$$

where $\boldsymbol{R}_i(\phi_i)$ is the rotation matrix of the local coordinate o_i–$x_iy_iz_i$ with respect to the global coordinate o-xyz with a rotation angle ϕ_i around the z-axis, which can be expressed by

$$\boldsymbol{R}_i(\phi_i)=\begin{bmatrix}\cos\phi_i & \sin\phi_i & 0\\ -\sin\phi_i & \cos\phi_i & 0\\ 0 & 0 & 1\end{bmatrix}, \tag{6}$$

$\boldsymbol{r}_i$ is the position vector of the point o_i expressed in the global coordinate. $\boldsymbol{S}_i(\boldsymbol{r}_i)$ represents the skew-symmetric operator for the vector $\boldsymbol{r}_i=[x_i,y_i,z_i]$ with the notation:

$$\boldsymbol{S}_i=\begin{bmatrix}0 & -z_i & y_i\\ z_i & 0 & -x_i\\ -y_i & x_i & 0\end{bmatrix}. \tag{7}$$

As is discussed above, there are seven key parameters needed to be determined during the modeling process, namely the dimension parameters b_i, w_i, and L, the position vector $\boldsymbol{r}_i=[x_i, y_i, z_i]$ and the rotation angle ϕ_i of the CTM.

As for the straight-axis flexure hinges, the rotation angle ϕ_i will be zero. The dimension parameters are $b_i=2f_b(x_i)$, $w_i=2f_w(x_i)$ and $L=l/N$. In view of the single- directional flexure hinges with just variable width, b_i will be constant, i.e. $b_i=b_0$. The position vector will be $\boldsymbol{r}_i=[x_i, 0, 0]$.

In view of the circle-axis flexure hinges, b_i is constant. w_i can be derived in terms of the geometry model of the circular-axis flexure hinges presented in ref. [35]. Unlike the straight-axis flexure hinges, this sort of hinges will be uniformly divided in terms of the center angle θ_m. The model parameters can be determined by

$$\begin{cases} \phi_i = \theta_i, \\ L = R\theta_m / N, \\ \boldsymbol{r}_i = [R\sin\theta_i, R(1-\cos\theta_i), 0]. \end{cases} \tag{8}$$

For the number of the divided pieces N, it is definite that larger N will lead to more accurate results. Since the matrix computation process is computationally efficient, it will be a good solution to just choose a large enough value of N to obtain accurate enough results. In this paper, N is set as 1000.

3 Compliance modeling verification

To verify the efficiency and the accuracy of the proposed method, the compliance matrices of two typical sorts of straight-axis flexure hinges including the elliptical-arc-fillet flexure hinges [10,18] and the power-function-shaped flexure hinges [13,17] are investigated, and the results are compared with the ones obtained by conventional methods. Besides, a newly reported two-segment circular-axis symmetric notch flexure hinge [35] and a family of bi-axis flexure hinges with both variable width and variable thickness [40–42] are also modeled and validated to demonstrate the feasibility of the proposed modeling method for flexure hinges with much more complicated shapes.

3.1 Compliance matrices of typical flexure hinges

3.1.1 Case 1: Elliptical-arc-fillet flexure hinges

Chen et al. [10,18] proposed a sort of the generalized elliptical-arc-fillet flexure hinge which is illustrated in Figure 2, where a, b, t, l and θ_m are dimensional parameters of the flexure hinge, governing the geometric feature. By choosing specified parameters, various types of flexure hinges, such as elliptical (E) types, elliptical arc (EA) types, elliptical fillet (EF) types, elliptical arc fillet (ECF) types, right circular (RC) types, circular (C) types, circular fillet (CF) types and so on, can be obtained. More details about this sort of flexure hinges and the geometric models can be found in refs. [10,18].

To investigate the accuracy of the proposed modeling method for this class of flexure hinges, the compliance matrices obtained by the FBMM are compared with the analytical results obtained in refs. [10,18]. During the calculation process, the modulus of elasticity and the modulus of rigidity are chosen as 2.07×10^{11} and 8.1×10^{10} N/m^2, respectively. The thickness is chosen to be 10 mm. The other dimensional parameters are detailed in Table 1. The first three types are from ref. [10], and the rests are from ref. [18]. Results obtained by Chen et al. [10,18] as well as the FBMM method are presented in Table 2 denoting as (C) and (Z), respectively. Since the global coordinates are not the same, only the absolute values are adopted to make comparisons.

From the results shown in Table 2, except for α_x/M_x of the first three hinges, almost all the compliance results are equal, and only very slight deviations (<0.1%) can be observed for a small number of terms of the compliance matrix. The good agreement demonstrates that the FBMM method is not only simple but also accurate. As for the term α_x/M_x, much larger deviations are observed which may be caused by the complex torsional effects. For further analysis, the finite element analysis results reported in ref. [10] and the relative errors of the analytical results of α_x/M_x of the first three hinges are presented in Table 3. As shown in Table 3, significant improvement of the modeling accuracy is achieved. The results demonstrate that the modified compliance matrix shown in eq. (1) is more accurate, and it is more suitable to describe the elastic deformation behavior of flexure hinges.

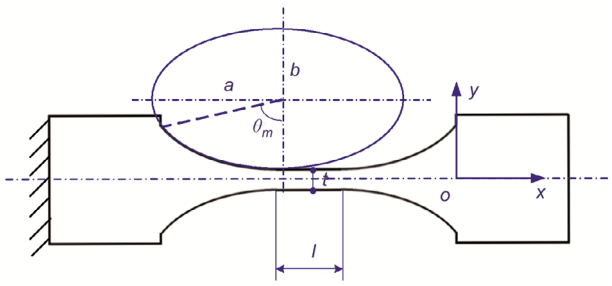

Figure 2 Schematic of the typical elliptical-arc-fillet flexure hinge.

Table 1 Dimensional parameters of the elliptical-arc-fillet flexure hinges

	a (mm)	b (mm)	l (mm)	t (mm)	θ_m	Type
1	7.071	4	0	1	45°	EA
2	5.774	4	0	1	60°	EA
3	5	4	0	1	90°	E
4	4	3	2	0.2	90°	EF
5	4	3	2	0.2	60°	EAF
6	3	3	0	0.2	90°	RC
7	3	3	2	0.2	60°	C
8	3	3	2	0.2	60°	CF

Table 2 Comparison results for refs. [10,18] (C) and the proposed modeling method (Z) (in SI units)

	$\Delta x/F_x$	$\Delta y/F_y$	$\Delta z/F_z$	α_x/M_x
1 (C)	3.211×10^{-9}	6.535×10^{-7}	2.155×10^{-8}	1.752×10^{-2}
1 (Z)	3.211×10^{-9}	6.536×10^{-7}	2.155×10^{-8}	1.606×10^{-2}
2 (C)	2.481×10^{-9}	5.240×10^{-7}	1.884×10^{-8}	1.445×10^{-2}
2 (Z)	2.481×10^{-9}	5.239×10^{-7}	1.884×10^{-8}	1.325×10^{-2}
3 (C)	2.565×10^{-9}	4.471×10^{-7}	1.684×10^{-8}	1.255×10^{-2}
3 (Z)	2.565×10^{-9}	4.472×10^{-7}	1.684×10^{-8}	1.151×10^{-2}
4 (C)	1.120×10^{-8}	6.051×10^{-5}	7.128×10^{-8}	–
4 (Z)	1.120×10^{-8}	6.052×10^{-5}	7.128×10^{-8}	–
5 (C)	1.107×10^{-8}	4.872×10^{-5}	6.343×10^{-8}	–
5 (Z)	1.107×10^{-8}	4.873×10^{-5}	6.344×10^{-8}	–
6 (C)	4.777×10^{-9}	6.035×10^{-6}	2.014×10^{-8}	–
6 (Z)	4.777×10^{-9}	6.047×10^{-6}	2.015×10^{-8}	–
7 (C)	4.681×10^{-9}	4.559×10^{-6}	1.840×10^{-8}	–
7 (Z)	4.681×10^{-9}	4.561×10^{-6}	1.840×10^{-8}	–
8 (C)	4.777×10^{-9}	2.896×10^{-5}	4.551×10^{-8}	–
8 (Z)	4.777×10^{-9}	2.896×10^{-5}	4.551×10^{-8}	–
	α_y/M_y	α_z/M_z	$\Delta y/M_z$	$\Delta z/F_y$
1 (C)	3.853×10^{-4}	2.311×10^{-2}	1.156×10^{-4}	1.926×10^{-6}
1 (Z)	3.853×10^{-4}	2.311×10^{-2}	1.156×10^{-4}	1.927×10^{-6}
2 (C)	3.409×10^{-4}	1.904×10^{-2}	9.522×10^{-5}	1.705×10^{-6}
2 (Z)	3.409×10^{-4}	1.904×10^{-2}	9.522×10^{-5}	1.705×10^{-6}
3 (C)	3.078×10^{-4}	1.652×10^{-2}	8.262×10^{-5}	1.539×10^{-6}
3 (Z)	3.078×10^{-4}	1.652×10^{-2}	8.263×10^{-5}	1.539×10^{-6}
4 (C)	1.344×10^{-3}	2.234	1.162×10^{-2}	6.720×10^{-6}
4 (Z)	1.344×10^{-3}	2.234	1.162×10^{-2}	6.721×10^{-6}
5 (C)	1.329×10^{-3}	2.323	1.037×10^{-2}	5.931×10^{-6}
5(Z)	1.329×10^{-3}	2.323	1.037×10^{-2}	5.932×10^{-6}
6 (C)	5.732×10^{-4}	0.656	1.967×10^{-3}	1.720×10^{-6}
6 (Z)	5.732×10^{-4}	0.656	1.967×10^{-3}	1.721×10^{-6}
7 (C)	5.617×10^{-4}	0.132	1.704×10^{-3}	1.459×10^{-6}
7 (Z)	5.617×10^{-4}	0.132	1.704×10^{-3}	1.460×10^{-6}
8 (C)	1.141×10^{-3}	2.105	7.574×10^{-3}	4.107×10^{-6}
8 (Z)	1.141×10^{-3}	2.105	7.574×10^{-3}	4.107×10^{-6}

Table 3 Comparisons of α_x/M_x between FEA (F) and analytical results (in SI units)

	1		2		3	
	Value	error	value	error	value	error
F	1.383×10^{-2}		1.178×10^{-2}		1.634×10^{-2}	
C	1.445×10^{-2}	5.2%	1.255×10^{-2}	6.5%	1.752×10^{-2}	7.2%
Z	1.325×10^{-2}	4.2%	1.151×10^{-2}	2.3%	1.606×10^{-2}	1.7%

3.1.2 Case 2: Power function shaped fillet flexure hinges

The typical power function shaped fillet flexure hinge is shown in Figure 3. The shape of this sort of flexure hinge is the combination of a circle arc and a power function shaped arc which are tangential at the connective point, and it can be regarded as a typical example of the newly developed multi- segment flexure hinges [29,31]. Generally, the governing equation of the power function arc can be expressed as $y=(ax+p)^n$. When the exponent is set as n=1, the V-shaped fillet flexure hinge can be obtained [12,13]. To investigate the sufficiency of the proposed modeling method for flexure hinges with various structure features, both analytical and FEA results of the V- shaped fillet flexure hinges with ten series of dimensional parameters covering wide ranges of both the ratios R/t and the circle angles in ref. [13] are employed for comparisons, the specified calculation parameters and the comparison results are given in Table 4. As for the power function shaped fillet flexure hinges, four arbitrary series of dimensional parameters of this type of flexure hinges as presented in Table 5 are employed as the testing objects. During the calculation process, the modulus of elasticity and the Poisson's ratio are set as 2.07×10^{11} N/m^2

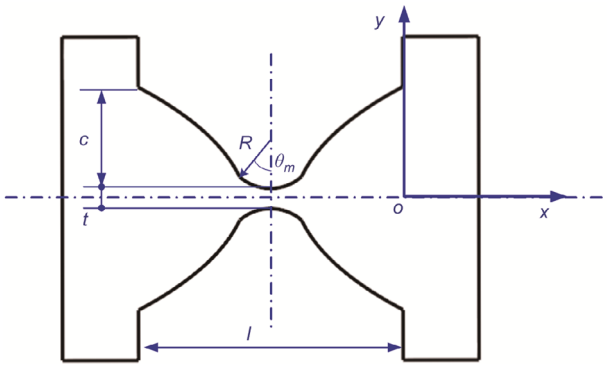

Figure 3 Schematic of the power function shaped fillet flexure hinge.

Table 4 Comparing results for ref. [13] (T) and the proposed modeling method (Z) (in SI units)

R (mm)	θ_m (°)	t (mm)	Stiffness ($\times10^{-5}$ m/N)		
			Analy. (T)	Analy. (Z)	FEA
2	15	1	7.2653	7.2075	6.7824
4	30	1	7.3202	7.2710	6.7146
6	45	1	6.0704	6.0348	5.6638
8	60	1	5.2144	5.1853	4.9317
10	75	1	4.6223	4.5970	4.4131
2	15	0.5	1.5454	1.5413	1.4710
4	30	0.5	1.3136	1.3110	1.2534
6	45	0.5	1.0729	1.0709	1.0366
8	60	0.5	0.9244	0.9227	0.9001
10	75	0.5	0.8229	0.8214	0.8058
2	15	0.2	0.1787	0.1786	0.1736
4	30	0.2	0.1332	0.1331	0.1306
6	45	0.2	0.1085	0.1084	0.1071
8	60	0.2	0.0937	0.0937	0.0929
10	75	0.2	0.0837	0.0837	0.0838

The Young's modulus and the Poisson's ratio are set as 210 GPa and 0.28, respectively.

Table 5 Dimensional parameters of the power function shaped fillet flexure hinges

	n	r (mm)	t (mm)	c (mm)	θ_m
1	0.3	3	0.2	9.9	45°
2	0.5	6	0.5	9.75	45°
3	0.7	9	0.8	9.6	60°
4	0.9	12	1	9.5	60°

and 0.288, respectively. The thickness is chosen as 10 mm. The reference results are calculated according to the closed-form compliance equations provided in ref. [17], the comparison results are then given in Table 6.

As shown in Table 4, the compliance results obtained by the FBMM method are slightly smaller than the referred analytical results, but they are more accurate when comparing with the FEA results. Take the first one as an example where R/t=2, the relative error in ref. [13] (T) is about 7.12% while that obtained here is about 6.41%, validating the improvement of accuracy of the result obtained by the proposed FBMM method. Moreover, with the increase of R/t, the two sorts of analytical results will become much closer to each other as well as the FEA results. When R/t> 30, the analytical results obtained by the two methods become equal. The comparisons demonstrate that the proposed modeling method is more accurate, and it is also more universal for flexure hinges with various structure features. Comparisons in Table 6 show that most of the compliance results obtained by the two modeling method have good agreements, while much larger deviations can be observed as for the terms $\Delta z/F_z$ and $\Delta y/F_y$, which may be caused by the difference of the employed shear coefficients. All the results well demonstrate the feasibility and the accuracy of the proposed FBMM method for modeling flexure hinges with various structure features.

3.2 Compliance matrices of flexure hinges with more complicated shapes

3.2.1 Case 3: Two-segment circular-axis symmetric notch flexure hinges

The typical structure of a two-segment circular-axis symmetric notch flexure hinge proposed by Lobontiu and Cullin [35] is illustrated in Figure 1(a), which is a planar compliance with a circular axis and variable in plane sections. By means of Castigliano's second theorem, the modeling process is introduced in ref. [35]. In this paper, this type of flexure hinges is investigated to verify the sufficiency of the proposed modeling method for more complicated flexure hinges.

To have a comparison with the analytical results shown in ref. [35], the same material and shape parameters are employed in this paper. As for the material, the modulus of elasticity and the Poisson's ratio are set as 2.07×10^{11} N/m^2 and 0.33, respectively. As for the flexure hinge, the thickness is chosen to be 6.35 mm, the dimensional parameters shown in Figure 1(a) are set as follows: t=1.5113 mm, r_1=9.8951 mm, r_2=13.339 mm, θ_m=8°, R=81.75 mm. The comparison results are specified in Table 6. From the results shown in Table 7, the two sets of analytical results are almost the same, the good agreement between the two analytical results demonstrate the efficiency and accuracy of the proposed modeling method for this sort of flexure hinges.

Table 6 Comparisons results for ref. [17] (L) and the proposed modeling method (Z) (in SI units)

	α_z/M_z	α_z/F_y	$\Delta z/M_y$	$\Delta z/F_z$
1 (L)	6.428×10^{-1}	6.428×10^{-3}	5.957×10^{-6}	7.691×10^{-8}
1 (Z)	6.459×10^{-1}	6.460×10^{-3}	5.958×10^{-6}	7.723×10^{-7}
2 (L)	9.167×10^{-2}	9.167×10^{-4}	5.155×10^{-6}	6.685×10^{-8}
2 (Z)	9.225×10^{-2}	9.226×10^{-4}	5.155×10^{-6}	6.848×10^{-8}
3 (L)	3.486×10^{-2}	3.486×10^{-4}	4.805×10^{-6}	6.403×10^{-8}
3 (Z)	3.488×10^{-2}	3.488×10^{-4}	4.805×10^{-6}	6.574×10^{-8}
4 (L)	2.301×10^{-2}	2.301×10^{-4}	4.774×10^{-6}	6.727×10^{-8}
4 (Z)	2.307×10^{-2}	2.307×10^{-4}	4.787×10^{-6}	6.720×10^{-8}
	$\Delta y/M_z$	$\Delta y/F_y$	$\Delta x/F_x$	
1 (L)	6.446×10^{-3}	6.429×10^{-5}	4.964×10^{-9}	
1 (Z)	6.460×10^{-3}	6.474×10^{-5}	4.964×10^{-9}	
2 (L)	9.167×10^{-4}	9.181×10^{-6}	4.296×10^{-9}	
2 (Z)	9.226×10^{-4}	9.323×10^{-6}	4.296×10^{-9}	
3 (L)	3.486×10^{-4}	3.494×10^{-6}	4.133×10^{-9}	
3 (Z)	3.488×10^{-4}	3.576×10^{-6}	4.004×10^{-9}	
4 (L)	2.301×10^{-4}	2.315×10^{-6}	3.978×10^{-9}	
4 (Z)	2.307×10^{-4}	2.402×10^{-6}	3.988×10^{-9}	

3.2.2 Case 4: Bi-axis flexure hinges

A typical sort of bi-axis flexure hinges with variable profiles along both the x-axis and the z-axis is illustrated in Figure 1(c). As shown in Figure 1(c), it possesses two compliant axes due to the unique axially-collocated notches. The governing parameters for its geometric features are also illustrated in Figure 1(c). Generally, the notches can be elliptical curves [40], right circle curves [41], or parabolic curves [42]. More details about the moving principles and the structure features of the flexure hinges can refer to refs. [40–42]. Although the unique structures will provide the designers more compact structures and more feasible design process, the more complicated shapes will require more efforts to model its elastic deformation behavior. In this paper, all the three types of bi-axis flexure hinges are modeled by the proposed FBMM method, and the results are compared with analytical results obtained by the Castigliano's second theorem [40–42]. The employed material parameters and structure parameters are shown in Table 8, and the comparison results are further shown in Table 9. In Table 9, the results for elliptical curves (BE), right circle

Table 7 Comparison results for ref. [35] (L) and the proposed method (Z) (in SI units)

	$\Delta x/F_x$	$\Delta x/F_y$	$\Delta y/F_x$
L	4.382×10^{-8}	3.765×10^{-7}	3.765×10^{-7}
Z	4.381×10^{-8}	3.682×10^{-7}	3.682×10^{-7}
	$\Delta x/M_z$	α_z/F_x	$\Delta y/F_y$
L	3.055×10^{-5}	3.055×10^{-5}	5.011×10^{-6}
Z	3.055×10^{-5}	3.055×10^{-5}	5.013×10^{-6}
	$\Delta y/M_z$	α_z/F_y	α_z/M_z
L	4.211×10^{-4}	4.211×10^{-4}	3.703×10^{-2}
Z	4.213×10^{-4}	4.213×10^{-4}	3.704×10^{-2}

curves (BC), and parabolic curves (BP) in previous work are denoted by (CJ) [40], (C) [41], and (L) [42], respectively, while the results obtained by FEA method and the proposed modeling method are denoted by (FEA) and (Z), respectively.

From the results shown in Table 9, it can be seen that the values of the terms $\Delta y/F_y$ and $\Delta z/F_z$ obtained by the proposed modeling method are much larger than the values in previous research work. It is due to the reason that the shearing effects are ignored in previous work, while the shearing terms are included in eq. (1), resulting in the increase of the values. The rest compliance components of the first four types of flexure hinges are equal. As for the parabolic shaped bi-axis flexure hinges, the FEA results are also employed from ref. [42]. By supposing the FEA results to be the accurate ones, the relative errors are also given in Table 9, whereby it can be seen that the relative errors of the proposed modeling method are about half of the ones obtained in ref. [42] except for the above-mentioned terms. The results well indicate that the proposed modeling method is not only more convenient but also more accurate than the conventional modeling methods.

Table 8 Dimensional parameters of the bi-axis flexure hinges

	E (N/m^2)	μ	t (mm)	w (mm)	c_t (mm)	c_w (mm)	l (mm)	Type
1	2.1×10^{11}	0.25	1	1.5	5	5	10	BC
2	2.2×10^{11}	0.28	3.2	4.1	9	9	18	BC
3	2.1×10^{11}	0.25	2	3	8	10	60	BE
4	2.2×10^{11}	0.28	1	1.5	4	6	30	BE
5	2.0×10^{11}	0.3	0.4	0.6	1	1.5	2.5	BP

Table 9 Comparison results of the bi-axis flexure hinges [40–42] (in SI units)

	α_z/M_z	$\Delta y/F_y$	$\Delta y/M_z$	$\Delta z/F_z$
1 (C)	8.60×10^{-2}	2.235×10^{-6}	4.302×10^{-4}	1.103×10^{-6}
1 (Z)	8.60×10^{-2}	2.273×10^{-6}	4.307×10^{-4}	1.138×10^{-6}
2 (C)	2.10×10^{-2}	1.839×10^{-7}	1.924×10^{-5}	1.194×10^{-7}
2 (Z)	2.10×10^{-2}	1.926×10^{-7}	1.926×10^{-5}	1.280×10^{-7}
3 (CJ)	3.51×10^{-2}	3.304×10^{-5}	0.0011	1.539×10^{-5}
3 (Z)	3.51×10^{-2}	3.316×10^{-5}	0.0011	1.548×10^{-5}
4 (CJ)	0.2626	6.167×10^{-5}	0.0039	2.741×10^{-5}
4 (Z)	0.2626	6.190×10^{-5}	0.0039	2.756×10^{-5}
5 (FEA)	1.68	2.85×10^{-3}	2.1×10^{-3}	1.00×10^{-6}
5 (L)	1.76	3.01×10^{-3}	2.2×10^{-3}	1.06×10^{-6}
5 (Z)	1.72	3.08×10^{-3}	2.2×10^{-3}	1.40×10^{-6}
5 Error (L)	4.54%	5.31%	4.50%	5.66%
5 Error (Z)	2.38%	8.07%	4.50%	40.0%
	$\Delta z/F_y$	α_y/M_y	$\Delta x/F_x$	
1 (C)	2.107×10^{-4}	0.0421	1.136×10^{-8}	
1 (Z)	2.109×10^{-4}	0.0421	1.137×10^{-8}	
2 (C)	1.242×10^{-5}	0.0014	2.753×10^{-9}	
2 (Z)	1.243×10^{-5}	0.0014	2.753×10^{-9}	
3 (CJ)	4.889×10^{-4}	0.0163	1.795×10^{-8}	
3 (Z)	4.895×10^{-4}	0.0163	1.796×10^{-8}	
4 (CJ)	0.0018	0.1167	3.300×10^{-8}	
4 (Z)	0.0018	0.1167	3.301×10^{-8}	
5 (FEA)	9.20×10^{-4}	7.40×10^{-1}	2.90×10^{-8}	
5 (L)	9.70×10^{-4}	7.76×10^{-1}	3.04×10^{-8}	
5 (Z)	9.45×10^{-4}	7.56×10^{-1}	3.00×10^{-8}	
5 Error (L)	5.15%	4.64%	4.61%	
5 Error (Z)	2.72%	2.16%	3.45%	

4 Conclusions

In this paper, a novel finite beam based matrix modeling (FBMM) method is proposed to numerically obtain the compliance matrices of flexure hinges with complicated shapes. The main concept of the method is to treat the flexure hinges as serial connections of finite micro-beams. By means of matrix calculations, compliance matrices of flexure hinges can be derived effectively without dealing with numerous integral operations. To demonstrate the sufficiency of this method, the basic compliance matrices of two typical sorts of flexure hinges and another two sorts of flexure hinges with more complicated shapes are calculated and compared with the corresponding results reported before.

As for the compliance results of all the flexure hinges obtained by the proposed modeling method, most of them have good agreements with the analytical results obtained by conventional modeling methods. However, there is little deviation between the results of the compliance terms as for the V-shaped fillet flexure hinges and the parabolic shaped bi-axis flexure hinges, further comparisons with finite element analysis results indicate that the proposed method is of higher modeling accuracy. The results demonstrate that the proposed FBMM method is not only simple but also accurate.

This work was supported by the National Natural Science Foundation of China (Grant Nos. 50775099, 51075041, 51175221 and 51305162).

1 Zhu Z, Zhou X, Liu Z, et al. Development of a piezoelectrically actuated two-degree-of-freedom fasttool servo with decoupled motions for micro-/nanomachining. Precis Eng, 2014, 38: 809–820
2 Zhu Z, Zhou X, Liu Q, et al. Multi-objective optimum design of fast tool servo based on improved differential evolution algorithm. J Mech Sci Tech, 2011, 25: 3141–3149
3 Zubir M N M, Shirinzadeh B, Tian Y. Development of a novel flexure-based microgripper for high precision micro-object manipulation. Sensor Actuator Phys, 2009, 150: 257–266
4 Li Y, Xu Q. A totally decoupled piezo-driven *XYZ* flexure parallel micropositioning stage for micro/nanomanipulation. IEEE T Autom Sci Eng, 2011, 8: 265–279
5 Li Y, Huang J, Tang H. A compliant parallel *XY* micromotion stage with complete kinematic decoupling. IEEE T Autom Sci Eng, 2012, 9: 538–553
6 Yong Y, Moheimani S, Kenton B, et al. Invited Review Article: High-speed flexure-guided nanopositioning: Mechanical design and control issues. Rev Sci Instrum, 2012, 83: 121101–121122
7 Wu Y, Zhou Z. Design calculations for flexure hinges. Rev Sci In-

strum, 2002, 73: 3101–3106
8 Lobontiu N, Paine J S N, Garcia E, et al. Corner-filleted flexure hinges. J Mech Des, 2001, 123: 346–352
9 Koseki Y, Tanikawa T, Koyachi N, et al. Kinematic analysis of translational 3-DOF micro parallel mechanism using matrix method. In: Proceedings 2000 IEEE/RSJ International Conference on Intelligent Robots and Systems. Takamatsu, 2000. 786–792
10 Chen G, Shao X, Huang X. A new generalized model for elliptical arc flexure hinges. Rev Sci Instrum, 2008, 79: 095103–095108
11 Smith S T, Badami V G, Dale J S, et al. Elliptical flexure hinges. Rev Sci Instrum, 1997, 68: 1474–1483
12 Tian Y, Shirinzadeh B, Zhang D, et al. Three flexure hinges for compliant mechanism designs based on dimensionless graph analysis. Precis Eng, 2010, 34: 92–100
13 Tian Y, Shirinzadeh B, Zhang D. Closed-form compliance equations of filleted V-shaped flexure hinges for compliant mechanism design. Precis Eng, 2010, 34: 408–418
14 Chen G, Liu X, Gao H, et al. A generalized model for conic flexure hinges. Rev Sci Instrum, 2009, 80: 055106–055110
15 Lobontiu N, Paine J S, O'Malley E, et al. Parabolic and hyperbolic flexure hinges: flexibility, motion precision and stress characterization based on compliance closed-form equations. Precis Eng, 2002, 26: 183–192
16 Lobontiu N, Paine J S, Garcia E, et al. Design of symmetric conic-section flexure hinges based on closed-form compliance equations. Mech Mach Theor, 2002, 37: 477–498
17 Li Q, Pan C, Xu X. Closed-form compliance equations for power-function-shaped flexure hinge based on unit-load method. Precis Eng, 2013, 37: 135–145
18 Chen G, Liu X, Du Y. Elliptical-arc-fillet flexure hinges: Toward a generalized model for commonly used flexure hinges. J Mech Des, 2011, 133: 081002
19 Lobontiu N, Garcia E, Hardau M, et al. Stiffness characterization of corner-filleted flexure hinges. Rev Sci Instrum, 2004, 75: 4896–4905
20 Shusheng B, Shanshan Z, Xiaofeng Z. Dimensionless design graphs for three types of annulus-shaped flexure hinges. Precis Eng, 2010, 34: 659–666
21 Yong Y, Moheimani S. Design of an Inertially counterbalanced Z-nanopositioner for high-speed atomic force microscopy. IEEE Trans Nanotechnol, 2013, 12: 137–145
22 Zelenika S, Munteanu M G, De Bona F. Optimized flexural hinge shapes for microsystems and high-precision applications. Mech Mach Theor, 2009, 44: 1826–1839
23 Linß S, Erbe T, Zentner L. On polynomial flexure hinges for increased deflection and an approach for simplified manufacturing. In: 13th World Congress in Mechanism and Machine Science. Guanajuato, México, 2011
24 Yong Y K, Lu T F. The effect of the accuracies of flexure hinge equations on the output compliances of planar micro-motion stages. Mech Mach Theor, 2008, 43: 347–363
25 Yong Y K, Lu T F, Handley D C. Review of circular flexure hinge design equations and derivation of empirical formulations. Precis Eng, 2008, 32: 6–70
26 Eastman F S. Flexure Pivots to Replace Knife Edges and Ball Bearings: An Adaptation of Beam-Column Analysis. Washington: University of Washington, 1935.
27 Paros J M, Weisbord L. How to design flexure hinges. Mach Des, 1965, 37: 151–156
28 Marsh D. The construction and performance of various flexure hinges. J Sci Instrum, 1962, 39: 493
29 Lobontiu N, Cullin M, Petersen T, et al. planar compliances of symmetric notch flexure hinges: The right circularly corner-filleted parabolic design. IEEE Trans Autom Sci Eng, 2014, 11: 169–176
30 Vallance R R, Haghighian B, Marsh E R. A unified geometric model for designing elastic pivots. Precis Eng, 2008, 32: 278–288
31 Lobontiu N, Cullin M, Ali M, et al. A generalized analytical compliance model for transversely symmetric three-segment flexure hinges. Rev Sci Instrum, 2011, 82: 105116–105119
32 Li Y, Xu Q. Design and analysis of a totally decoupled flexure-based XY parallel micromanipulator. IEEE Trans Robot, 2009, 25: 645–657
33 Tang H, Li Y. Design, Analysis, and Test of a novel 2-DOF nanopositioning system driven by dual mode. IEEE Trans Robot, 2013, 29: 650–662
34 Pham H H, Chen I. Stiffness modeling of flexure parallel mechanism. Precis Eng, 2005, 29: 467–478
35 Lobontiu N, Cullin M. In-plane elastic response of two-segment circular-axis symmetric notch flexure hinges: The right circular design. Precis Eng, 2013, 37: 542–555
36 Kang D, Gweon D. Analysis and design of a cartwheel-type flexure hinge. Precis Eng, 2012, 37: 33–43
37 Cowper G. The shear coefficient in Timoshenko's beam theory. J Appl Mech, 1966, 33: 335–340
38 Chen G, Howell L L. Two general solutions of torsional compliance for variable rectangular cross-section hinges in compliant mechanisms. Precis Eng, 2009, 33: 268–274
39 Li Y, Xu Q. Development and assessment of a novel decoupled XY parallel micropositioning platform. IEEE ASME Trans Mech, 2010, 15: 125
40 Cao F, Jiao Z X. Design of double-axis elliptical flexure hinges (In Chinese). Eng Mech, 2007, 24: 178–182
41 Chen A, Cao F, Hou W. The flexibility calculation of biaxial right circular flexible hinge. J Basic Sci Eng, 2010, 5: 015
42 Lobontiu N, Garcia E. Two-axis flexure hinges with axially-collocated and symmetric notches. Comput Struct, 2003, 81: 1329–1341